Crystal structure of cariprazine dihydrochloride, $C_{21}H_{34}Cl_2N_4OCl_2$

James A. Kaduk,[1,2,a] Megan M. Rost,[3] Anja Dosen,[3] and Thomas N. Blanton[3]
[1]*Illinois Institute of Technology, 3101 S. Dearborn St., Chicago, IL 60616, USA*
[2]*North Central College, 131 S. Loomis St., Naperville, IL 60540, USA*
[3]*ICDD, 12 Campus Blvd., Newtown Square, PA 19073-3273, USA*

(Received 20 June 2024; accepted 10 September 2024)

The crystal structure of cariprazine dihydrochloride has been solved and refined using synchrotron X-ray powder diffraction data and optimized using density functional theory techniques. Cariprazine dihydrochloride crystallizes in space group $P2_1/n$ (#14) with $a = 27.26430(14)$, $b = 7.29241(1)$, $c = 12.80879(4)$ Å, $\beta = 99.5963(2)°$, $V = 2511.038(8)$ Å^3, and $Z = 4$ at 295 K. The crystal structure consists of layers of cations parallel to the *bc*-plane. The cations stack along the *b*-axis. Each H atom on the two protonated N atoms participates in a discrete N–H···Cl hydrogen bond. One Cl anion acts as an acceptor in two of these bonds, while the other Cl is an acceptor in only one bond. The result is to link the cations and anions into columns parallel to the *b*-axis. The powder pattern has been submitted to the ICDD for inclusion in the Powder Diffraction File™ (PDF®).

[doi:10.1017/S0885715624000526]

Key words: cariprazine, Vraylar, powder diffraction, Rietveld refinement, density functional theory

I. INTRODUCTION

Cariprazine, $C_{21}H_{32}N_4O$ (as the hydrochloride salt $C_{21}H_{33}N_4OCl$, marketed under the trade names Vraylar and Reagila, among others), is used in the treatment of a variety of psychological disorders including schizophrenia as well as manic depression or a combination of behaviors associated with bipolar disorder. Cariprazine is included in the Top 200 Small Molecule Drugs by Retail Sales in 2022 (McGrath et al., 2010). The systematic name of cariprazine hydrochloride (CAS Registry Number 1083076-69-0) is 3-[4-[2-[4-(2,3-dichlorophenyl)piperazin-1-yl]ethyl]cyclohexyl]-1,1-dimethylurea hydrochloride. A two-dimensional molecular diagram of the cariprazine dication is shown in Figure 1.

Cariprazine hydrochloride Form I was claimed in US Patent 7,943,621 B2 (Czibula et al., 2011; Richter Gideon). The dihydrochloride salt was also claimed, but we are unaware of any published powder diffraction data for the dihydrochloride. Form III of cariprazine hydrochloride is claimed in US Patent 7,829,569 B2 (Liao et al., 2010; Forest Laboratories).

This work was carried out as part of a project (Kaduk et al., 2014) to determine the crystal structures of large-volume commercial pharmaceuticals and include high-quality powder diffraction data for them in the Powder Diffraction File (Kabekkodu et al., 2024).

II. EXPERIMENTAL

Cariprazine hydrochloride was a commercial reagent, purchased from TargetMol (Batch #159104), and was used as-received. The white powder was packed into a 1.5 mm diameter Kapton capillary and rotated during the measurement at ~50 Hz. The powder pattern was measured at 295 K at beamline 11-BM (Antao et al., 2008; Lee et al., 2008; Wang et al., 2008) of the Advanced Photon Source at Argonne National Laboratory using a wavelength of 0.459744(2) Å from 0.5 to 40° 2θ with a step size of 0.001° and a counting time of 0.1 s/step. The high-resolution powder diffraction data were collected using 12 silicon crystal analyzers for high angular resolution, high precision, and accurate peak positions. A mixture of silicon (NIST SRM 640c) and alumina (NIST SRM 676a) standards (ratio Al_2O_3:Si = 2:1 by weight) was used to calibrate the instrument and refine the monochromatic wavelength used in the experiment.

The pattern was indexed using JADE Pro (MDI, 2023) on a very high-quality ($F(20) = 205$, JADE figure of merit = 6) primitive monoclinic unit cell with $a = 27.26552$, $b = 7.29133$, $c = 12.80730$ Å, $\beta = 99.60°$, $V = 2510.48$ Å^3, and $Z = 4$. The suggested space group was $P2_1/n$, which was confirmed by successful solution and refinement of the structure. A reduced cell search of the Cambridge Structural Database (Groom et al., 2016) yielded seven hits but no structures of cariprazine derivatives.

The structure was solved by direct methods using EXPO2014 (Altomare et al., 2013), invoking the COVMAP option. In addition to the cariprazine molecule and the Cl ion, the solution contained another atom, which was assigned as O62 (a water molecule?). The structure also contained a small void, which was filled by another O atom (O63). The occupancy of O63 refined to 0.11, and its position moved very close to Cl1, so it was removed from the refinement. The occupancy of O62 refined to 2.1, and it moved to a reasonable position for a second Cl ion, so it was renamed

[a]Author to whom correspondence should be addressed. Electronic mail: kaduk@polycrystallography.com

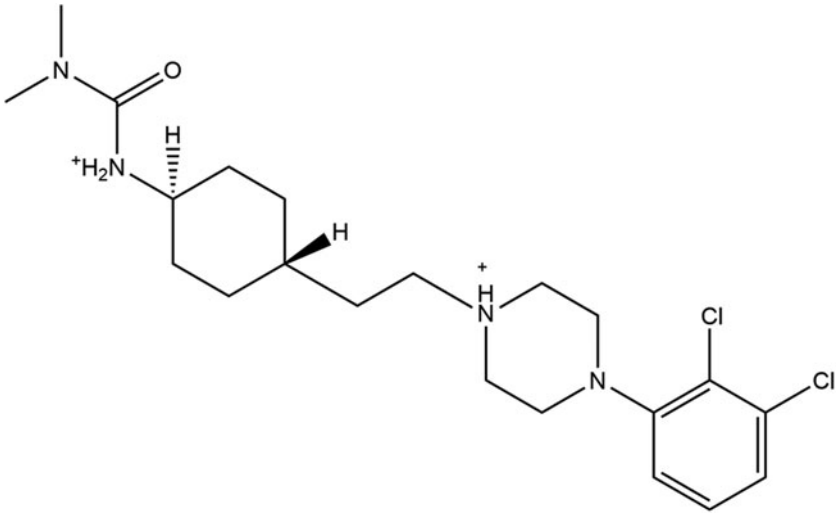

Figure 1. The 2-dimensional structure of the cariprazine dication.

Cl62. The compound is thus the dihydrochloride. H63 and H64 were added to N5 and N6, respectively, based on potential hydrogen bonds.

Rietveld refinement was carried out with GSAS-II (Toby and Von Dreele, 2013). Only the 1.9–25.0° portion of the pattern was included in the refinements ($d_{\min} = 1.062$ Å). All non-H-bond distances and angles were subjected to restraints based on a Mercury/Mogul Geometry Check (Bruno et al., 2004; Sykes et al., 2011). The Mogul average and standard deviation for each quantity were used as the restraint parameters. The restraints contributed 1.8% to the final χ^2. The hydrogen atoms were included in calculated positions, which were recalculated during the refinement using Materials Studio (Dassault, 2022). The Cl atoms were refined anisotropically. The U_{iso} of the C, N, and O atoms were grouped by chemical similarity. The U_{iso} for the H atoms were fixed at 1.3× the U_{iso} of the heavy atoms to which they are attached. The peak profiles were described using a uniaxial microstrain model, with 010 as the unique axis.

The final refinement of 136 variables using 23,137 observations and 71 restraints yielded the residuals $R_{wp} = 0.10797$ and goodness of fit = 1.68. The largest peak (0.10 Å from Cl3) and hole (0.74 Å from C13) in the difference Fourier map were 0.46(9) and −0.39(9) eÅ^{-3}, respectively. The final Rietveld plot is shown in Figure 2. The largest features in the normalized error plot represent subtle errors in peak positions and may represent changes in the specimen during the measurement.

The crystal structure of cariprazine dihydrochloride was optimized (fixed experimental unit cell) with density functional theory techniques using VASP (Kresse and Furthmüller, 1996)

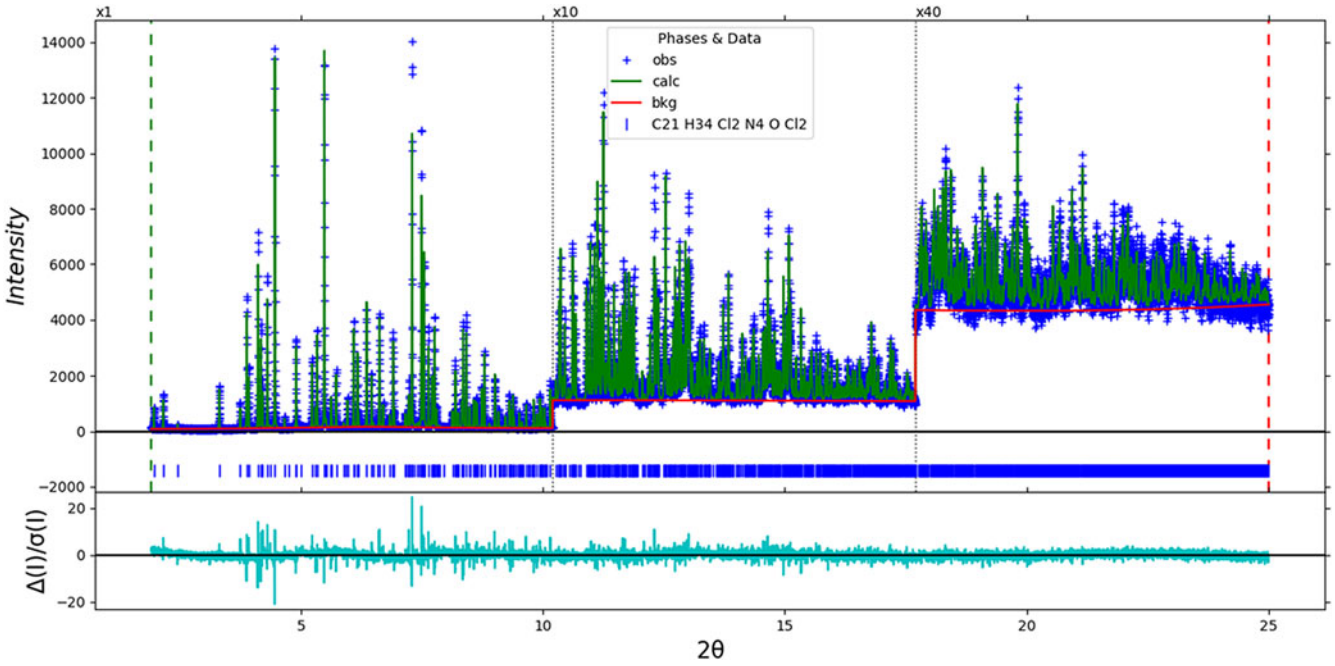

Figure 2. The Rietveld plot for the refinement of cariprazine dihydrochloride. The blue crosses represent the observed data points, and the green line is the calculated pattern. The cyan curve is the normalized error plot, and the red line is the background curve. The x-axis is degrees 2θ, and the y-axis is the reported counts. The vertical scale has been multiplied by a factor of 10× for $2\theta > 10.2°$ and by a factor of 40× for $2\theta > 17.7°$.

https://doi.org/10.1017/S0885715624000526 Published online by Cambridge University Press

through the MedeA graphical interface (Materials Design, 2016). The calculation was carried out on 16 2.4 GHz processors (each with 4 Gb RAM) of a 64-processor HP Proliant DL580 Generation 7 Linux cluster at North Central College. The calculation used the GGA-PBE functional, a plane wave cutoff energy of 400.0 eV, and a *k*-point spacing of 0.5 $Å^{-1}$, leading to a $2 \times 2 \times 1$ mesh, and took ~76.7 h. Single-point density functional calculations (fixed experimental cell) and population analysis were carried out using CRYSTAL23 (Erba et al., 2023). The basis sets for the H, C, N, and O atoms in the calculation were those of Gatti et al. (1994), and the basis set for Cl was that of Peintinger et al. (2013). The calculations were run on a 3.5 GHz PC using eight *k*-points and the B3LYP functional and took ~5.1 h.

III. RESULTS AND DISCUSSION

Despite being purchased as "cariprazine hydrochloride", the sample studied here is cariprazine dihydrochloride. The asymmetric unit (Figure 3) contains one cariprazine dication and two Cl anions. The root-mean-square Cartesian displacement of the non-H atoms in the Rietveld-refined and VASP-optimized cation structures is 0.188 Å (Figure 4). The agreement is within the normal range for correct structures (van de Streek and Neumann, 2014) and confirms that the structure is correct. The remainder of this discussion will emphasize the VASP-optimized structure.

Almost all of the bond distances, bond angles, and torsion angles fall within the normal ranges indicated by a Mercury Mogul Geometry check (Macrae et al., 2020). The torsion angles involving rotation about the C8–C9 bond are flagged as unusual. They lie on the tails of peaked 0/180° distributions and indicate that the orientation of the dimethylamino group is slightly unusual.

Quantum chemical geometry optimization of the isolated cation (DFT/B3LYP/6-31G*/water) using Spartan '20 (Wavefunction, 2022) indicated that the observed solid-state conformation is 8.9 kcal/mol higher in energy than a local minimum, which has an almost identical conformation. The global minimum-energy conformation (MMFF force field) is 4.2 kcal/mol lower in energy than the observed conformation and is less-linear. The difference indicates that intermolecular

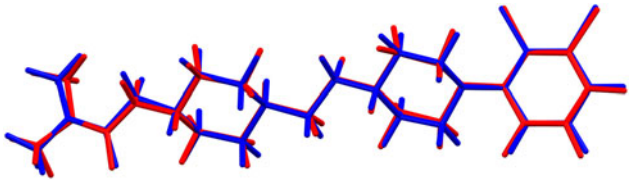

Figure 4. Comparison of the Rietveld-refined (red) and VASP-optimized (blue) structures of the cariprazine cation. The rms Cartesian displacement is 0.188 Å. Image generated using Mercury (Macrae et al., 2020).

interactions are important in determining the observed extended conformation.

The crystal structure (Figure 5) consists of layers of cations parallel to the *bc*-plane. The cations stack along the *b*-axis. The mean plane of the cation is approximately −11,−6,3. The Mercury Aromatics Analyser indicates two strong interactions between the dichlorophenyl rings in adjacent cations. Analysis of the contributions to the total crystal energy of the structure using the Forcite module of Materials Studio (Dassault Systèmes, 2022) suggests that bond, angle, and torsion distortion terms contribute about equally to the intramolecular energy. The intermolecular energy is dominated by electrostatic attractions, which, in this force field analysis, include hydrogen bonds. The hydrogen bonds are better analyzed using the results of the DFT calculation.

Each H atom on the two protonated N atoms (N5 and N6) participates in a discrete N–H···Cl hydrogen bond. Cl62 acts as an acceptor in two of these bonds, while Cl1 is an acceptor in only one (Table I). The result is to link the cations and anions into columns parallel to the *b*-axis. One C–H···O hydrogen bond links cations, and several C–H···Cl hydrogen bonds also link cations and anions. There is one intramolecular C–H···Cl hydrogen bond.

The volume enclosed by the Hirshfeld surface of cariprazine dihydrochloride (Figure 6, Hirshfeld, 1977; Spackman et al., 2021) is 618.14 $Å^3$, which represents 98.47% of the unit cell volume. The packing density is thus fairly typical. The only significant close contacts (red in Figure 6) involve the hydrogen bonds. The volume/non-hydrogen atom is larger than the usual at 20.9 $Å^3$, reflecting the presence of multiple Cl atoms in the compound.

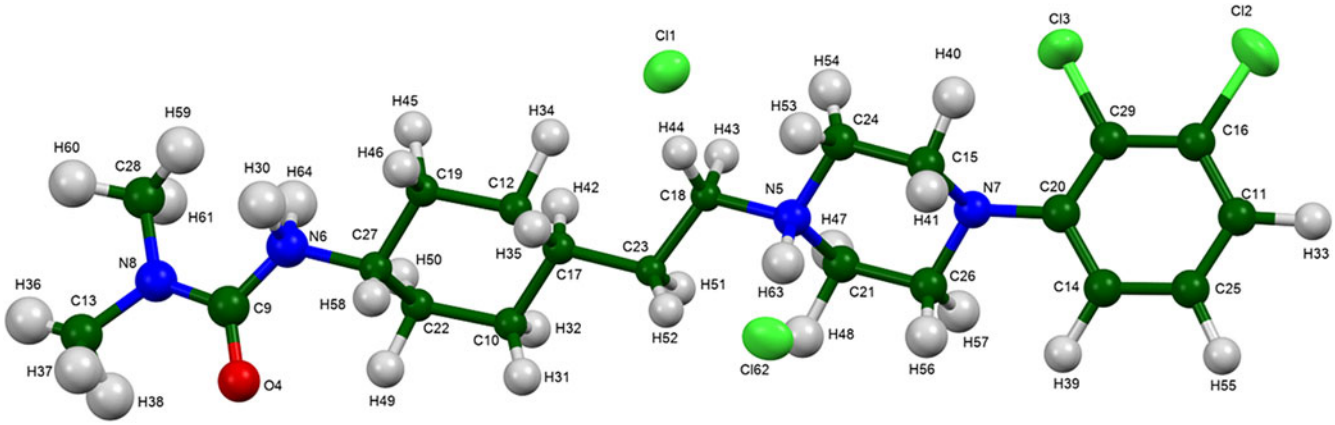

Figure 3. The asymmetric unit of cariprazine dihydrochloride, with the atom numbering. The atoms are represented by 50% probability spheroids/ellipsoids. Image generated using Mercury (Macrae et al., 2020).

https://doi.org/10.1017/S0885715624000526 Published online by Cambridge University Press

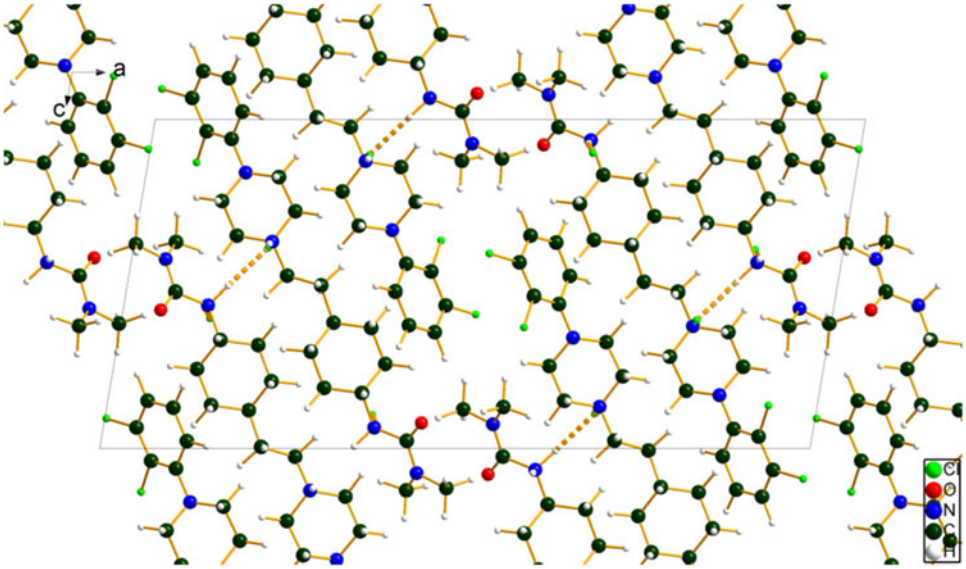

Figure 5. The crystal structure of cariprazine dihydrochloride is viewed down the *b*-axis. Image generated using Diamond (Crystal Impact, 2023).

TABLE I. Hydrogen bonds (CRYSTAL23) in cariprazine dihydrochloride.

H-bond	D–H (Å)	H···A (Å)	D···A (Å)	D–H···A (Å)	Overlap (*e*)
N6–H64···Cl1	1.104	1.893	2.984	169.0	0.126
N6–H30···Cl62	1.059	2.178	3.210	164.2	0.087
N5–H63···Cl62	1.067	2.091	3.155	175.4	0.097
C28–H61···O4	1.103	2.626	3.662	156.1	0.013
C28–H59···Cl62	1.094	2.715	3.593	137.0	0.018
C13–H38···Cl1	1.099	2.766	3.568	129.6	0.015
C26–H57···Cl62	1.099	2.805	3.638	132.4	0.023
C24–H54···Cl62	1.101	2.711	3.772	161.5	0.028
C22–H50···Cl1	1.101	2.666	3.568	138.8	0.014
C18–H44···Cl1	1.101	2.513	3.550	156.5	0.039
C18–H43···Cl62	1.102	2.862	3.873	152.6	0.020
C25–H55···Cl1	1.090	2.816	3.755	144.2	0.019
C15–H40···Cl3	1.096	2.540[a]	3.180	116.3	0.011

[a]Intramolecular.

The Bravais–Friedel–Donnay–Harker (Bravais, 1866; Friedel, 1907; Donnay and Harker, 1937) morphology suggests that we might expect elongated morphology for cariprazine dihydrochloride, with ⟨010⟩ as the long axis. A second-order spherical harmonic model was included in the refinement. The texture index was 1.019(0), indicating that the preferred orientation was slight in this rotated capillary specimen.

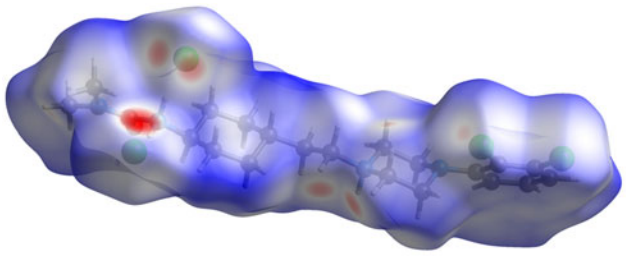

Figure 6. The Hirshfeld surface of cariprazine dihydrochloride. Intermolecular contacts longer than the sums of the van der Waals radii are colored blue, and contacts shorter than the sums of the radii are colored red. Contacts equal to the sums of radii are white. Image generated using CrystalExplorer (Spackman et al., 2021).

IV. DEPOSITED DATA

The powder pattern of cariprazine dihydrochloride from this synchrotron data set has been submitted to the ICDD for inclusion in the Powder Diffraction File. The Crystallographic Information Framework (CIF) files containing the results of the Rietveld refinement (including the raw data) and the DFT geometry optimization were deposited with the ICDD. The data can be requested at pdj@icdd.com.

ACKNOWLEDGEMENTS

Use of the Advanced Photon Source at Argonne National Laboratory was supported by the U. S. Department of Energy, Office of Science, Office of Basic Energy Sciences under Contract No. DE-AC02-06CH11357. This work was partially supported by the International Centre for Diffraction Data. We thank Saul Lapidus for his assistance in the data collection.

CONFLICTS OF INTEREST

The authors have no conflicts of interest to declare.

REFERENCES

Altomare, A., C. Cuocci, C. Giacovazzo, A. Moliterni, R. Rizzi, N. Corriero, and A. Falcicchio. 2013. "EXPO2013: A Kit of Tools for Phasing Crystal Structures from Powder Data." *Journal of Applied Crystallography* 46: 1231–5.

Antao, S. M., I. Hassan, J. Wang, P. L. Lee, and B. H. Toby. 2008. "State-of-the-Art High-Resolution Powder X-ray Diffraction (HRPXRD) Illustrated with Rietveld Refinement of Quartz, Sodalite, Tremolite, and Meionite." *Canadian Mineralogist* 46: 1501–9.

Bravais, A. 1866. *Etudes Cristallographiques*. Paris, Gauthier Villars.

Bruno, I. J., J. C. Cole, M. Kessler, J. Luo, W. D. S. Motherwell, L. H. Purkis, B. R. Smith, R. Taylor, R. I. Cooper, S. E. Harris, and A. G. Orpen. 2004. "Retrieval of Crystallographically-Derived Molecular Geometry

https://doi.org/10.1017/S0885715624000526 Published online by Cambridge University Press

Information." *Journal of Chemical Information and Computer Sciences* 44: 2133–44.
Crystal Impact. 2023. Diamond. V. 5.0.0. Crystal Impact - Dr. H. Putz & Dr. K. Brandenburg. Windows.
Czibula, L., F. Sebok, I. Greiner, G. Domany, and E. A. Csongor. 2011. "Salts of Piperazine Compounds as D3/D2 Antagonists." United States Patent 7.943,621 B2.
Dassault Systèmes. 2022. *Materials Studio 2023*. San Diego, CA, BIOVIA.
Donnay, J. D. H., and D. Harker. 1937. "A New Law of Crystal Morphology Extending the Law of Bravais." *American Mineralogist* 22: 446–67.
Erba, A., J. K. Desmarais, S. Casassa, B. Civalleri, L. Donà, I. J. Bush, B. Searle, L. Maschio, L.-E. Daga, A. Cossard, C. Ribaldone, E. Ascrizzi, N. L. Marana, J.-P. Flament, and B. Kirtman. 2023. "CRYSTAL23: A Program for Computational Solid State Physics and Chemistry." *Journal of Chemical Theory and Computation* 19: 6891–932. doi:10.1021/acs.jctc.2c00958.
Friedel, G. 1907. "Etudes sur la loi de Bravais." *Bulletin de la Société Française de Minéralogie* 30: 326–455.
Gatti, C., V. R. Saunders, and C. Roetti. 1994. "Crystal-Field Effects on the Topological Properties of the Electron-Density in Molecular Crystals - the Case of Urea." *Journal of Chemical Physics* 101: 10686–96.
Groom, C. R., I. J. Bruno, M. P. Lightfoot, and S. C. Ward. 2016. "The Cambridge Structural Database." *Acta Crystallographica Section B: Structural Science, Crystal Engineering and Materials* 72: 171–9.
Hirshfeld, F. L. 1977. "Bonded-Atom Fragments for Describing Molecular Charge Densities." *Theoretica Chemica Acta* 44: 129–38.
Kabekkodu, S., A. Dosen, and T. N. Blanton. 2024. "PDF-5+: A Comprehensive Powder Diffraction File™ for Materials Characterization." *Powder Diffraction* 39: 47–59.
Kaduk, J. A., C. E. Crowder, K. Zhong, T. G. Fawcett, and M. R. Suchomel. 2014. "Crystal Structure of Atomoxetine Hydrochloride (Strattera), $C_{17}H_{22}NOCl$." *Powder Diffraction* 29: 269–73.
Kresse, G., and J. Furthmüller. 1996. "Efficiency of Ab-Initio Total Energy Calculations for Metals and Semiconductors Using a Plane-Wave Basis Set." *Computational Materials Science* 6: 15–50.
Lee, P. L., D. Shu, M. Ramanathan, C. Preissner, J. Wang, M. A. Beno, R. B. Von Dreele, L. Ribaud, C. Kurtz, S. M. Antao, X. Jiao, and B. H. Toby. 2008. "A Twelve-Analyzer Detector System for High-Resolution Powder Diffraction." *Journal of Synchrotron Radiation* 15: 427–32.
Liao, X., H. Zhu, and A. Grill. 2010. "Solvate and Crystalline Forms of Carbamoyl-Cyclohexane Derivatives." United States Patent 7.829,569 B2.
Macrae, C. F., I. Sovago, S. J. Cottrell, P. T. A. Galek, P. McCabe, E. Pidcock, M. Platings, G. P. Shields, J. S. Stevens, M. Towler, and P. A. Wood. 2020. "*Mercury 4.0*: From Visualization to Design and Prediction." *Journal of Applied Crystallography* 53: 226–35.
Materials Design. 2016. *MedeA 2.20.4*. Angel Fire, NM, Materials Design Inc.
McGrath, N. A., M. Brichacek, and J. T. Njardarson. 2010. "A Graphical Journey of Innovative Organic Architectures That Have Improved Our Lives." *Journal of Chemical Education* 87 (12): 1348–49. doi:10.1021/ed1003806.
MDI. 2023. *JADE Pro Version 8.3*. Livermore, CA, Materials Data.
Peintinger, M. F., D. Vilela Oliveira, and T. Bredow. 2013. "Consistent Gaussian Basis Sets of Triple-Zeta Valence with Polarization quality for Solid-State Calculations." *Journal of Computational Chemistry* 34: 451–9.
Spackman, P. R., M. J. Turner, J. J. McKinnon, S. K. Wolff, D. J. Grimwood, D. Jayatilaka, and M. A. Spackman. 2021. "Crystalexplorer: A Program for Hirshfeld Surface Analysis, Visualization and Quantitative Analysis of Molecular Crystals." *Journal of Applied Crystallography* 54: 1006–11. doi:10.1107/S1600576721002910.
Sykes, R. A., P. McCabe, F. H. Allen, G. M. Battle, I. J. Bruno, and P. A. Wood. 2011. "New Software for Statistical Analysis of Cambridge Structural Database Data." *Journal of Applied Crystallography* 44: 882–6.
Toby, B. H., and R. B. Von Dreele. 2013. "GSAS II: The Genesis of a Modern Open Source All Purpose Crystallography Software Package." *Journal of Applied Crystallography* 46: 544–9.
van de Streek, J., and M. A. Neumann. 2014. "Validation of Molecular Crystal Structures from Powder Diffraction Data with Dispersion-Corrected Density Functional Theory (DFT-D)." *Acta Crystallographica Section B: Structural Science, Crystal Engineering and Materials* 70: 1020–32.
Wang, J., B. H. Toby, P. L. Lee, L. Ribaud, S. M. Antao, C. Kurtz, M. Ramanathan, R. B. Von Dreele, and M. A. Beno. 2008. "A Dedicated Powder Diffraction Beamline at the Advanced Photon Source: Commissioning and Early Operational Results." *Review of Scientific Instruments* 79: 085105.
Wavefunction, Inc. 2022. *Spartan '20. V. 1.1.4*. Irvine, CA: Wavefunction Inc.

https://doi.org/10.1017/S0885715624000526 Published online by Cambridge University Press